Q. J. R. Meteorol. Soc. (2003), **129**, pp. 715–727 doi: 10.1256/qj.02.42

Determination of airflow across the Alpine ridge by a combination of airborne Doppler lidar, routine radiosounding and numerical simulation

By OLIVER REITEBUCH[1]*, HANS VOLKERT[1], CHRISTIAN WERNER[1], ALAIN DABAS[2], PATRICIA DELVILLE[3], PHILIPPE DROBINSKI[4], PIERRE H. FLAMANT[5] and EVELYNE RICHARD[6]

[1]*Institut für Physik der Atmosphäre, DLR, Oberpfaffenhofen, Germany*
[2]*CNRM, Météo-France, Toulouse, France*
[3]*Institut National des Sciences de L'Univers, Division Technique, Meudon, France*
[4]*Service d'Aéronomie, Université Pierre et Marie Curie, Paris, France*
[5]*Laboratoire de Météorologie Dynamique (LMD), CNRS, Palaiseau, France*
[6]*Laboratoire d'Aérologie, CNRS and Université Paul Sabatier, Toulouse France*

(Received 4 February 2002; revised 28 August 2002)

SUMMARY

The Wind Infrared Doppler lidar (WIND) instrument was flown on board the aircraft Falcon of the Deutsches Zentrum für Luft- und Raumfahrt on two missions during the Special Observing Period (SOP) of the Mesoscale Alpine Programme (MAP). During the first flight two complete sections of horizontal wind speed and direction were sampled up to a height of 7 km from Innsbruck to the Po basin and back. From the second mission 11 WIND soundings from 11 km downwards are presented along a route from a jet stream of up to 45 m s^{-1} above Berlin towards the Alps. A routine radiosounding from Milano and episode-type simulations with the Meso-NH modelling system are used for detailed comparisons and to obtain comparative statistics.

KEYWORDS: High-resolution simulation Jet stream Mesoscale Alpine Programme Valley flow

1. INTRODUCTION

The determination of atmospheric flow at different heights is a basic requirement in meteorology, both scientifically for the documentation and understanding of flow structures, and operationally, as an important input parameter for numerical weather-prediction models. Traditionally, wind profiles, i.e. the variation of horizontal wind speed and direction with height, are evaluated at discrete intervals from the drift of ascending balloons carrying radiosondes for pressure, temperature and humidity measurements. Large gaps in time (typically 6 to 12 h between ascents) and space (about 100 km between European regular radiosonde stations) are inevitable. More recently, surface-based wind profilers started to provide quasi-continuous (half hourly) wind profiles through microwave remote sensing above their location. Airborne remote-sensing techniques open the additional spatial dimension of the aircraft's track and allow the retrieval of the wind field in a two-dimensional plane. Optical techniques with Doppler lidars have the potential to sense the clear-air and partially cloudy atmosphere by measuring the movements of aerosol particles, whereas Doppler radars detect moving hydrometeors within clouds and precipitation areas.

The determination of the wind field via the observation of aerosol motion with an airborne laser system is technologically demanding and highly ambitious (Targ *et al.* 1996; Rothermel *et al.* 1998). The Wind Infrared Doppler lidar (WIND) instrument is so far the only airborne Doppler lidar for atmospheric research capable of retrieving wind profiles in a vertical plane below the aircraft with a conical scanning technique. It was used for the first time in a field campaign during the Special Observing Period (SOP) of the Mesoscale Alpine Programme (MAP, Bougeault *et al.* 2001).

The purpose of this concise study is to demonstrate the capabilities of the new instrument in two quite different meteorological settings and to compare the measured

* Corresponding author: Deutsches Zentrum für Luft- und Raumfahrt (DLR), Institut für Physik der Atmosphäre, Oberpfaffenhofen, D-82230 Wessling, Germany. e-mail: Oliver.Reitebuch@dlr.de

data with numerical simulation results as a proxy for independent validation data. Section 2 gives some technical background to the instrument and the retrieval technique, while section 3 briefly introduces the model and the case-study simulations. Section 4 presents the data for the Alpine flow on 11 October 1999 and the comparison of airborne Doppler lidar with numerical models for that case, and a jet-stream case on the day after. The final section discusses the results, and points to the next steps towards future applications of WIND.

2. The Doppler-lidar instrument WIND

The airborne Doppler-lidar WIND was developed in a French–German cooperation between the Centre National de la Recherche Scientifique (CNRS), the Centre National d'Etudes Spatiales (CNES), and the Deutsches Zentrum für Luft- und Raumfahrt (DLR). WIND measures the three-dimensional wind vector in a plane below the aircraft with a vertical resolution of 250 m. The system is operated on the DLR research aircraft Falcon, a twin-engine jet with a pressurized cabin and a maximum cruising altitude of 13 km.

The instrument is based on a coherent Doppler lidar with heterodyne detection at a wavelength of 10.6 μm (Vaughan *et al.* 1996; Pearson and Collier 1999). The system comprises a pulsed carbon dioxide (CO_2) laser and a continuous-wave CO_2 laser, a telescope, a scanning device and an optical mixing unit (Werner *et al.* 2001). The laser pulses are transmitted through the telescope, the scanning device, and a fuselage window into the atmosphere below the aircraft. A small portion of the light is backscattered by aerosols and cloud particles. The wavelength of the outgoing laser pulse is slightly shifted due to the Doppler effect on the backscattering particles, which move with the mean wind. This very small wavelength shift, which is of the order of magnitude of 10^{-8} compared with the outgoing laser pulse wavelength, is analysed with an optical heterodyne device. This yields the wind speed in the line-of-sight (LOS) direction of the transmitted laser pulse.

The wind profile is obtained by conically scanning around the vertical axis with a fixed angle of 30° from nadir with a Velocity Azimuth Display (VAD) scan (Browning and Wexler 1968). The profile of the three-dimensional wind vector can be calculated from the profiles of the LOS wind speeds with a sine-wave fitting procedure. This requires the assumption of horizontal homogeneity of the wind field in the plane of the scan. Two hundred LOS wind profiles are obtained during the 20 s of one scanner revolution and used for the sine-wave fitting procedure. It is necessary to average measurements of several scanner revolutions under conditions with low backscattered signal to improve the accuracy. An automatic quality-control algorithm discards unreliable wind velocities due to several criteria, e.g. for signal-to-noise ratio or percentage of outliers of LOS winds in the sine-fit procedure. The backscattered signal depends on the energy of the transmitted laser pulse as well as on the aerosol content of the atmosphere and the range of the measurement volume from the plane. Heavy aerosol loadings in the atmosphere are favourable for lidar measurements at the chosen wavelength. Measurements within clouds and below thick cloud layers are not feasible, because of strong extinction of the laser energy. Nevertheless, observations during partly cloudy conditions are possible, when the very thin laser beam of 1–3 m diameter is pointing through holes in the cloud layer.

The height resolution of 250 m is determined by the nadir angle and the laser pulse length, which varies from 1 to 3 μs. The horizontal resolution is defined by the cycloidal scan pattern, which is a function of the nadir angle, averaging period and aircraft ground

speed. The cross-track width of the cycloid amounts to 8 km at a height of 1 km for a flight altitude of 8 km and 30° nadir angle. The along-track horizontal resolution defines the separation of successive wind profiles and depends on the aircraft ground speed, the number of averaged scanner revolutions and the time period for one revolution. It amounts to 4 km per scanner revolution for typical values of 200 m s^{-1} aircraft speed and 20 s scanning period.

The major part of the Doppler shift of the returned signal is caused by the aircraft movement and only a minor part is due to the atmospheric wind. Therefore, it is necessary to determine the aircraft ground speed and attitude angles with high accuracy, which is achieved by a combination of data from an Inertial Reference System, a Global Positioning System, and the Doppler shift of the ground return.

Ground-based tests and comparitive measurements with radiosondes were performed during 1998–2000. The system was operated for the very first time on board an aircraft in June 1999. The respective retrievals of the wind vector and the results of the ground and airborne validations with data from radiosondes, a wind-profiler radar and the numerical model of Deutscher Wetterdienst are reported in Reitebuch *et al.* (2001).

3. The mesoscale simulation model

The simulations carried out here for cross validation, in the sense of Hollingsworth (1994), are obtained with the three-dimensional non-hydrostatic model Meso-NH, developed jointly by Météo-France and Laboratoire d'Aérologie. The model integrates a system of the primitive-equations based upon an anelastic formulation. The equations are integrated in a system of curvilinear coordinates with non-uniform grids: geographic conformal projections on the horizontal plane, and a height-based terrain-following vertical coordinate, which follows the topography. Lateral boundaries are prescribed as radiative or open. The top boundary is a rigid horizontal lid associated with an absorbing layer to prevent the reflection of gravity waves. The model contains a number of physical packages to reproduce the different atmospheric processes: a detailed soil scheme, a turbulent scheme based on the prediction of the turbulent kinetic energy, and detailed parametrizations for cloud and radiative processes. More details can be found in Lafore *et al.* (1998) and Stein *et al.* (2000).

Model simulations are performed with 80 vertical levels to the model top at 25 km with a vertical mesh stretched from 50 m at the ground to 500 m above 10 km. A two-way nesting strategy with a 10 km grid embedded within a 50 km grid was applied. The initial and boundary conditions are provided by either the analyses from the French Action de Recherche Petite Echelle Grande Echelle (ARPEGE) global model or the European Centre for Medium-Range Weather Forecasts (ECMWF) global model for the different situations (as specified in the next section). In essence the model is applied in this study as a consistent physical interpolator of the large-scale analysis providing a dynamical adaptation to a finer-scale orography, as the integration period for the model amounted to only two hours (12 to 14 UTC). A 10 km model horizontal resolution was chosen for the inner grid to achieve the best comparability with resolution of the Doppler lidar. The general ability of Meso-NH to reliably simulate cross-Alpine wave situations as well as gap flows down to the scale of the Wipp valley between Brenner and Innsbruck is documented in Volkert *et al.* (2003) and Flamant *et al.* (2002), respectively.

4. Measurements versus simulations results

During the MAP SOP the Falcon aircraft experienced a strong competition between different payloads, which could not be operated simultaneously due to space and

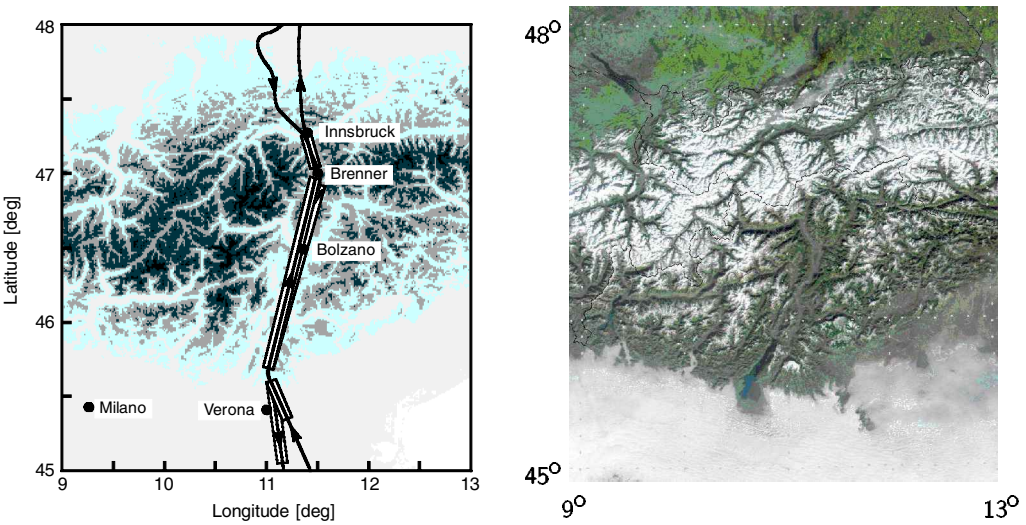

Figure 1. Massifs and deep valleys of the central Alps characterized by a digital elevation model with the Falcon track on 11 October 1999 superimposed (left) and as seen with snow above about 1500 m by a high-resolution satellite sensor (right, Moderate Resolution Imaging Spectroradiometer (MODIS) data of 2 February 2002; processing onto stereographic plane courtesy of G. Gesell, DLR). The width of the white bars of the flight track (left) indicates the diameter of the scanning cone at an altitude of 1 km, where Wind Infrared Doppler lidar (WIND) data are retrieved.

weight restrictions. For WIND a period had been pre-assigned which turned out to be governed by calm weather, during which no Intensive Observing Period (IOP) for all experimental surface stations was declared. Nevertheless, two successful Falcon missions were carried out. The first one across the Alps and along the major topographic incision south of their main ridge (the Adige valley and Garda Lake), and the second one between the Alps and northern Germany in the vicinity of a jet stream. The emphasis is placed on the low-wind Alpine case, while a statistical comparison over a larger range of speeds also takes into account the second case.

(*a*) *Flow across the Alps*

Measurements across the Alpine ridge were taken on 11 October 1999 from a flight altitude of 8 km above sea level (ASL) during a southbound flight leg from Innsbruck, over the Brenner pass and Bolzano, following the Adige valley, over Verona and the northern part of the Po basin and a corresponding northbound leg back (Fig. 1).

At upper levels the weather situation is characterized by a high-pressure system over northern Africa with slack westerly to north-westerly synoptic-scale winds over the Alpine region in a cloud-free atmosphere with high visibility. North of the Alps, the low-level flow is blocked by the mountains and follows their baseline. South of the Alps over Sardinia and Corsica, a surface high-pressure region (1026 hPa) induces south-westerly winds across the wide Po basin up to about 700 to 500 hPa.

The upstream conditions of the flow are well characterized by the routine noon sounding at Milano (Fig. 2). The wind profile shows a speed maximum in the surface layer. Above 1.5 km, the speed increases monotonically with a quasi-regular variation superimposed. Such variations are also apparent in the profile of wind direction, and quite subtly in the vertical gradient of potential temperature, i.e. atmospheric stability.

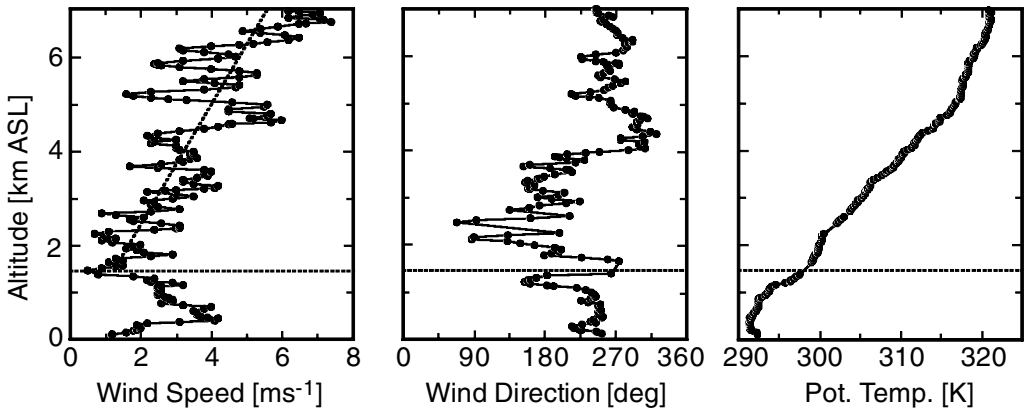

Figure 2. Routine radiosounding at Milano, upstream of the Alps, on 11 October 1999, 12 UTC: wind speed (left), wind direction (middle), and potential temperature (right). The dotted horizontal line at 1.5 km separates the surface layer from a region of monotonic increase in wind speed (inclined dashed line) with a quasi-regular variation superimposed. Dots designate individual data points.

Two simple physical inferences about the flow situation can be made from the sounding. First, an estimate of the Froude number (Fr) amounts to $Fr = 0.1$ with typical values of $U = 3$ m s^{-1}, $\theta = 297$ K, $\Delta\theta = 10$ K, $h = 2.5$ km, $N = 0.011$ s^{-1} for average wind speed, mean potential temperature, potential-temperature difference over one mountain height, mean mountain height, and average Brunt–Väisälä frequency, respectively. Such a low value of Fr indicates a blocking of the flow by the Alps below an estimated 'splitting height' of $z_s = h(1 - 2Fr) = 2$ km, as postulated by Hunt and Snyder (1980) from laboratory experiments. Second, the regular variations with height of wind speed and wind direction much resemble inertia-gravity waves as documented by radiosoundings within the stratosphere (e.g. Dörnbrack *et al.* 1999) with an estimated vertical wavelength of $\lambda = 2\pi U/N \approx 1.7$ km. We will see to what extent the simulation results and the remotely sensed winds corroborate these inferences from the routine sounding combined with simple physical settings.

Two vertical cross-sections of the flow above the Alps from the lidar measurements and one from the model simulation are juxtaposed in Fig. 3. Horizontal wind speed and direction data are retrieved for the southbound leg (1317–1349 UTC; Fig. 3, top row) and the northbound return leg (1356–1414 UTC; Fig. 3, middle row). The model data (Fig. 3, bottom row) are interpolated to the flight-track coordinates for 14 UTC from a simulation run, initialized with ARPEGE analyses at 12 UTC. Lidar profiles are obtained by averaging LOS data from three scanner revolutions (60 s), which corresponds to a horizontal resolution of 13 km for 215 m s^{-1} aircraft ground speed. The retrieval of wind profiles below the summit height of adjacent mountains using the VAD method necessitates special care, as the diameter of the scanning cone amounts to 8 km (see section 2). Therefore, no wind profiles are calculated here within valleys of a scale smaller than the diameter of the cycloid scan pattern.

The airborne Doppler lidar WIND apparently catches important features of the synoptic-scale flow and its modification by the Alps: (1) the horizontal shear in wind direction between the regions north and south of the Alps up to a height of 6 km, (2) the blocking and deflection of the low-level flow across the Po basin by the Alps as a whole, and most important (3) the characteristics of the flow in the Adige valley towards the main Alpine crest.

Specifically, in both sections the WIND data exhibit directional shear from south to north and from upper to lower levels. Likewise, wind speed generally increases with height and from south to north. The highest wind velocities sampled are about 15 m s^{-1} at the 7 km level above the Alpine crest (Brenner pass). The pixel display of Fig. 3 highlights the resolution of the measurements: 13 km in the horizontal and 0.25 km in the vertical direction. White spots indicate locations where a reliable wind retrieval is not possible due to the low aerosol content of the atmosphere; they mainly lie in the interval from 4 to 6 km. South of Bolzano local wind-speed maxima are evident below 2 km, in both WIND sections as well as in the simulation. The latter produces enhanced values over a larger area, possibly due to the somewhat exaggerated width of the valley in the model orography at 10 km horizontal resolution. Altogether, measured and simulated sections, which are obtained completely independently from each other, are in remarkable accord.

However, a distinct difference between measurements and simulation is the 2 to 3 m s^{-1} higher observed wind speed between 1 and 3 km above the Po basin (x = 200 km to x = 250 km in Fig. 3) in both flight sections. This observed elevated wind maximum agrees well with the surface-layer maximum in the Milano sounding (Fig. 2).

Horizontal sections of the flow at two different altitudes (1.5 and 6 km) demonstrate how well the topographic influence on the synoptic-scale flow is represented by the simulation, and how the single vertical cross-section discussed above is embedded in the three-dimensional flow (Fig. 4). The systematic south–north gradients in wind speed and direction, as measured in the cross-section above 4 km, are present over the entire central Alpine region at a height of 6 km (Fig. 4, left panel with flow vectors at *every other* grid point in both directions). At the 1.5 km level, which is below the crest line of the model orography and the 'splitting height' z_s as estimated above, the flow appears indeed to be deflected by the Alps as a whole. Within the Adige valley and Garda Lake incision, which in the model orography gets exaggerated in width at the 10 km horizontal resolution, the flow is clearly channelled and accelerated towards the Alpine crest (Fig. 4, right panel with flow vectors at *every* grid point).

South of Bolzano complete wind profiles can be determined as measured in both over flights, and as simulated, because of the sufficient width of the Adige valley at this location, and an adequate signal-to-noise ratio through the entire atmosphere below the aircraft (Fig. 5). Within the valley a distinct southerly wind maximum of 8.3 m s^{-1} is apparent at a height of 1.4 km (1.1 km above the ground) both in the simulation and the measurement. The flow direction is aligned with the valley axis. Above the in-valley surface layer the measured and the simulated speed attains a minimum of 2 to 3 m s^{-1} in a height of 2.6 km. Collocated is a distinct change in direction from southerly below to westerly prevailing above. With increasing height the simulated wind speed increases monotonically, while the observed winds exhibit systematic variations around the modelled values, just as the vertically better resolved routine data from the Milano sounding (Fig. 2), which are separated in time by 2 h and in space by 200 km. Under the assumption of flow modification by a wave disturbance, as suggested above from the Milano data, the systematic differences in the wind-speed variations between both over flights can be explained by a variation with time during the 30 min between the two retrievals. The southerly valley wind regime within the Adige valley under fair weather conditions was documented before by Dosio *et al.* (2001); measurements of the interplay of a Garda lake breeze with the Adige valley wind at Trento are reported by Zardi *et al.* (1999).

The simulation shows weak northerly winds within the Wipp valley north of the Brenner pass (x = 25 km in Fig. 3) close to the ground and a strong change in direction

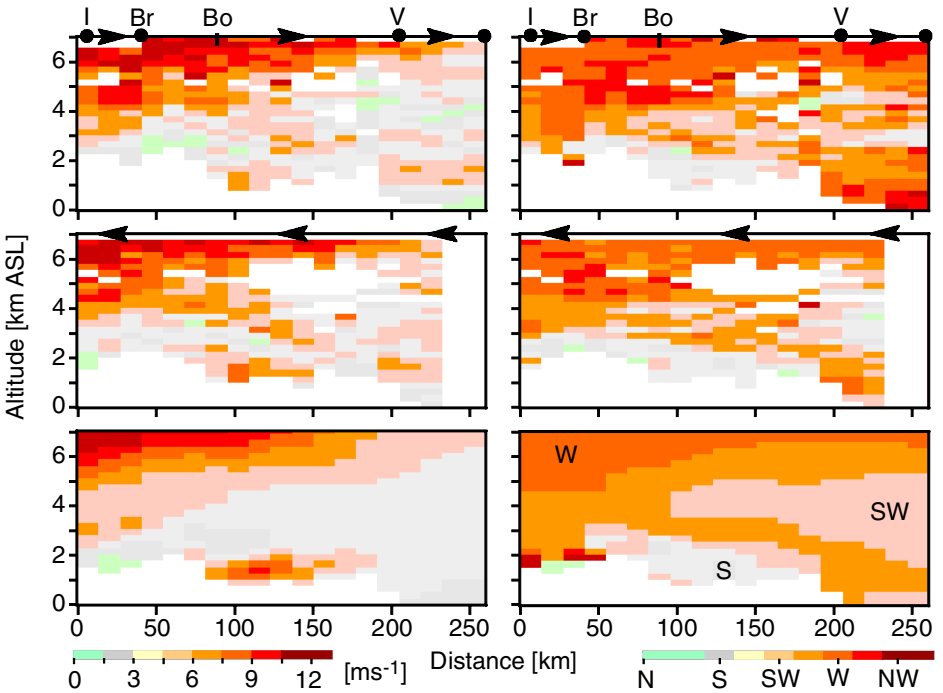

Figure 3. Alpine cross-sections on 11 October 1999 of horizontal wind speed (left column) and wind direction (conventional 22.5° sectors, right column) as measured by Wind Infrared Doppler lidar (WIND) on the southbound leg (top, 1317–1349 UTC), the northbound return leg (middle, 1356–1414 UTC), and as simulated by Meso-NH (bottom, 14 UTC). White pixels do not contain valid data, due to low aerosol content or underlying topography; arrows indicate flight direction. Geographic codes: Bo—Bolzano; Br—Brenner pass, I—Innsbruck; V—Verona.

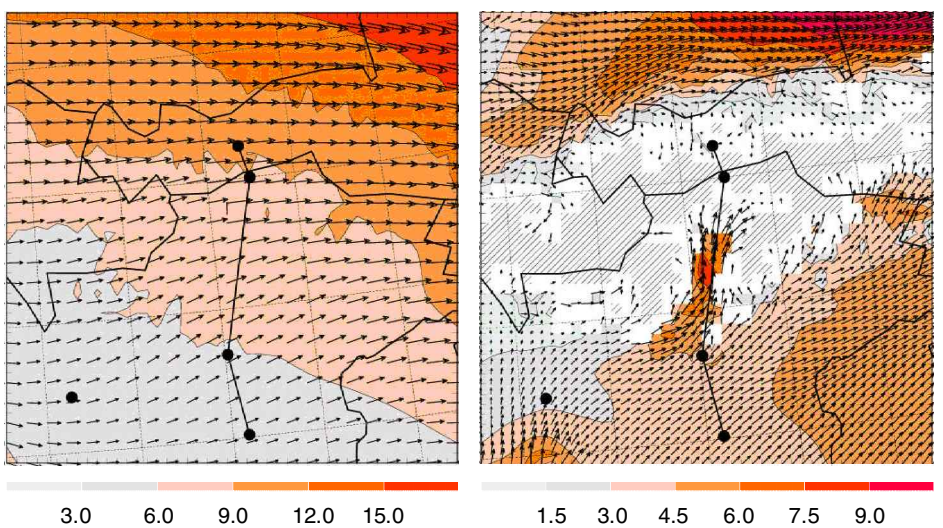

Figure 4. Horizontal sections of simulated horizontal wind velocity (m s^{-1}) at 6 km (left) and 1.5 km (right) for 11 October 1999, 14 UTC; colours (arrows) designate speed (direction). The meridional three-segment line indicates the position of the lidar measurements (cf. Figs. 1 and 3). In white regions valid data points are too sparse to analyse wind velocity because of the intersecting model orography, in the hatched region no wind vectors can be drawn. Geographic codes: Br—Brenner pass, I—Innsbruck; M—Milano sounding station; V—Verona.

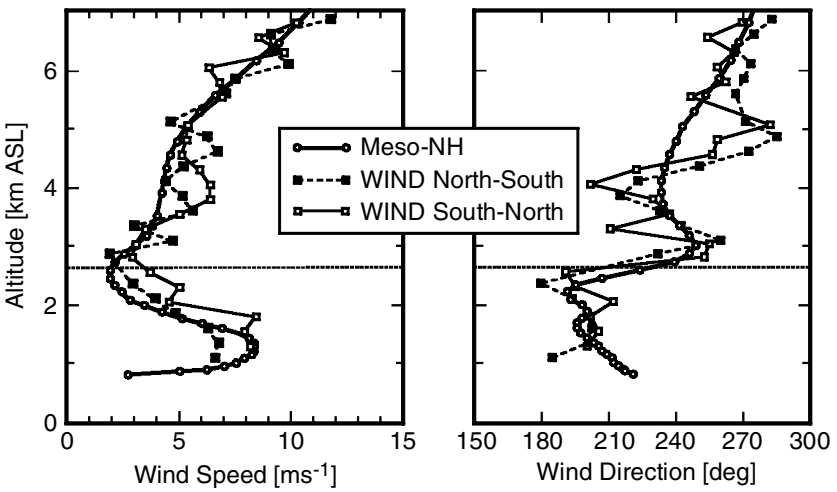

Figure 5. Comparison of measured and simulated wind profiles above the Adige valley just south of Bolzano (x = 100 km in Fig. 3) from the north-to-south leg (1336 UTC), the south-to-north return leg (1406 UTC) and the Meso-NH simulation (14 UTC). The horizontal line at 2.6 km separates the valley atmosphere below from the layer of quasi-monotonic speed increase above.

towards 240° at 2.5 km. WIND data could not be retrieved below 2 km within this narrow valley with the method applied here. A detailed analysis of the gap flow in the Wipp valley during a shallow south föhn event is reported by Flamant *et al.* (2002).

(*b*) *Comparative statistics*

A statistical comparison of the WIND measurements and Meso-NH simulations is performed in order to extend the previous study by Reitebuch *et al.* (2001). The data from the Alpine traverses discussed in the previous section are combined with those obtained during a jet-stream event north of the Alps on the day after. In such a way the sampled wind speeds range from 0 to 45 m s^{-1}. Additionally, two simulations of the jet-stream case are undertaken, initialized with ECMWF and ARPEGE global analyses, to check the sensitivity of the simulated mesoscale wind fields to different initial fields; this is of particular relevance as the simulations are only taken over 2 h.

On 12 October 1999, a strong jet stream with north-westerly winds higher than 50 m s^{-1} in the upper troposphere was situated over Denmark and northern Germany. A Falcon mission with WIND on board was undertaken to sample high wind speed in the vicinity of the Deutscher Wetterdienst profiling site at Lindenberg near Berlin. More details about the meteorological conditions and the Doppler lidar analysis of a jet streak within the jet stream can be found in Dabas *et al.* (2003).

Eleven WIND profiles, which were sampled from 1335 to 1354 UTC over a distance of about 230 km from Lindenberg towards the Alps, are presented in Fig. 6. The flight altitude was 11.3 km. Five scanner revolutions (100 s) had to be averaged to get one wind profile, which corresponds to an along-track resolution of about 22 km, and a 13 km across-track resolution on the ground. The retrievals are compared with the Meso-NH simulation for 14 UTC, which was initialized with the ECMWF analysis of 12 UTC. All profiles exhibit a strong vertical shear with maximum wind speed up to 45 m s^{-1} at an altitude of 10 km for the northernmost profiles. The wind speed at this altitude level is declining to 35 m s^{-1} for the last simulated profile, which is situated above the Erzgebirge range at the German–Czech border.

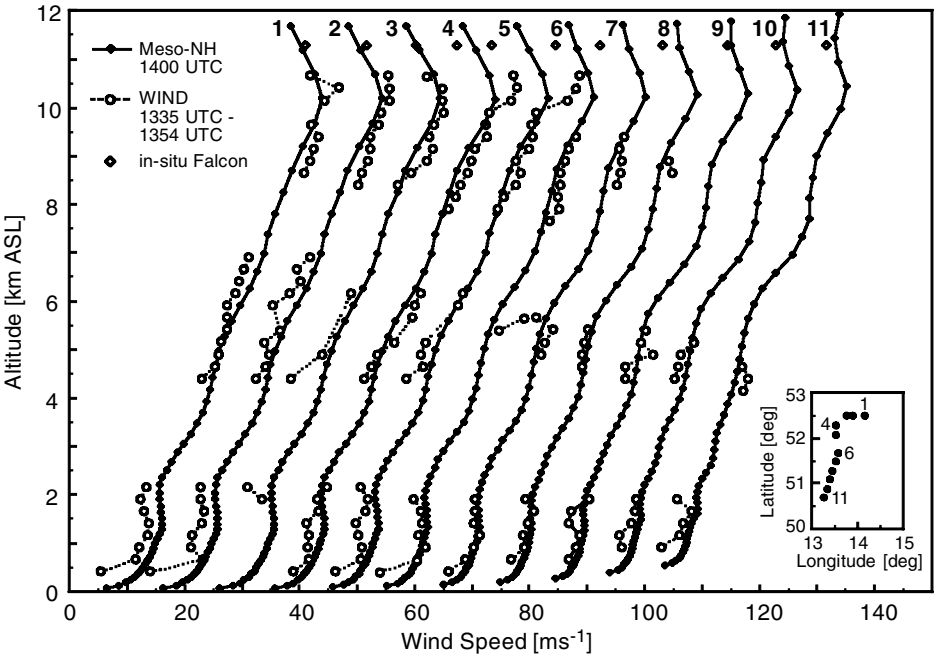

Figure 6. Sequence of 11 wind profiles from Lindenberg towards the south-west on 12 October 1999 (see inset for positions, profiles 2 to 11 shifted by 10 m s^{-1} relative to the previous one): measurements from the Wind Infrared Doppler lidar (WIND), where aerosol content is sufficiently high (open circles), versus Meso-NH simulation (filled diamonds at model levels, ECMWF initialization) and Falcon *in situ* measurements at 11.3 km with the five-hole pressure sonde of the nose boom (open diamonds).

The horizontal wind vector can be retrieved from WIND data from 300 m above ground to 600 m below the aircraft, except for altitudes between 2.5 to 4.5 km and 7 to 8 km. The signal-to-noise ratio is too low at these altitudes, due to the low amount of scattering aerosols. Above 8 km, ice crystals in cirrus clouds produced strong lidar signals in the first six profiles. The maximum altitude for reliable WIND values declines to about 5 km for the last three profiles, where no high-level clouds or aerosol layers were present.

For both the jet stream and the Alpine cases statistical scores are calculated, i.e. bias (systematic WIND mean minus simulation mean), root-mean-square difference (r.m.s.d., also called comparability), standard deviation (also called precision), relative standard deviation and correlation coefficient (normalized covariance; Table 1). The measured speed is systematically lower than the simulations for the jet-stream case especially for the range lower than 7 km (negative bias). The bias differs for the two initializations of the model as ECMWF initialized winds are up to 3 m s^{-1} lower at the jet-stream level of 10 km compared with corresponding values obtained from ARPEGE data. For the Alpine traverses the WIND measurements are slightly higher than the model results with a positive bias of 0.4 m s^{-1}. The wind direction shows no significant systematic difference between simulations and measurements. The r.m.s.d. value of 2.1 m s^{-1} is similar for the two different model runs of the jet-stream case but lower for the Alpine case. As wind speeds up to 45 m s^{-1} were measured during the jet-stream case, relative standard deviations below 10% and a very high correlation coefficient of 0.99 result, reflecting the fact that the strong speed increase with height is apparent in the measurements and the simulations. For the Alpine traverses with much more uniform

TABLE 1. STATISTICAL COMPARISON MEASURES FOR HORIZONTAL WIND SPEED AND DIRECTION DATA FROM WIND MEASUREMENTS VERSUS MESO-NH SIMULATIONS (ECMWF AND ARPEGE INITIALIZATIONS)

	Jet-stream case				Alpine traverses	
	ECMWF initialization		ARPEGE initialization		ARPEGE initialization	
	Speed	Direction	Speed	Direction	Speed	Direction
bias (m s^{-1}; deg.)	−0.4	2	−1.2	1	0.4	2
r.m.s.d. (m s^{-1}; deg.)	2.1	7	2.1	8	1.6	23
st. dev. (m s^{-1}; deg.)	2.1	7	1.7	7	1.5	23
relative st. dev. (%)	9	2	7	3	30	9
r	0.99	0.71	0.99	0.71	0.79	0.69
N	196	196	196	196	710	710

Systematic bias (WIND mean minus simulation mean); root-mean-square difference (r.m.s.d.), standard deviation (st. dev.), relative st. dev. (expressed as percentage of simulation mean), correlation coefficient (r) and total number of data pairs (N).

profiles of lower wind speeds, larger relative standard deviations of 30% and a reduced correlation coefficient of 0.79 are obtained. This difference in the correlation coefficient demonstrates the dependency on the range of the sampled values. The standard deviation of the wind direction of 23° is higher for the Alpine case compared with 7° for the jet-stream case. This is caused by the frequent presence of weak wind velocities below 2 m s^{-1}, where determination of the wind direction becomes increasingly ambiguous.

5. DISCUSSION AND CONCLUSION

The airborne Doppler lidar WIND was operated during the MAP SOP for the first time during a scientific field campaign. It was shown that this novel instrument has great potential for the study of dynamical processes, especially when the measured vertical cross-sections of the tropospheric flow below the aircraft can be combined with vertical and horizontal sections obtained from episode-type numerical simulations.

The cross-sections and the single soundings, as above Bolzano or from Lindenberg towards the Alps, show that in comparison with the independent simulations of similar spatial resolution WIND meets the performance requirements needed for mesoscale meteorology studies. The accuracy lies between 1 and 2 m s^{-1} and the vertical resolution amounts to 250 m. The derived statistical information for bias and standard deviation are in the range reported before for this instrument, but now with a higher level of confidence due to the larger dataset. While the vertical resolution is an instrumental constant, the horizontal resolution depends on the aeorosol content of the atmosphere, flight level, aircraft ground speed, and system performance. Significant improvements in horizontal resolution down to 3 km could be realized after the MAP SOP, when the WIND system took part in the campaign Expérience sur Site pour COntraindre les Modèles de Pollution atmosphérique et de Transport d'Emissions (ESCOMPTE) in southern France during summer 2001 (Dabas *et al.* 2002; for an overview see http://medias.obs-mip.fr/escompte, October 2002). This enhanced horizontal resolution is close to the grid size of a third inner nest of Meso-NH simulations (typically 2 km; e.g. Drobinski *et al.* 2003; Volkert *et al.* 2003).

The width of the conical scan pattern limits the resolution of measurements in the complex topography of Alpine valleys. The determination of along-valley winds or even the wind vector is in principle possible, when only data from sectors of a complete scan are analysed. Strong backscattered signals are needed for this approach, but the often

higher aerosol concentrations within valleys can favour such an attempt. Furthermore, higher horizontal resolution can be achieved with different scanning strategies like sideward looking in only one direction, or forward–backward scans to resolve wave-like structures (Drobinski *et al.* 2000), although at the expense of only being able to retrieve just one component of the wind vector.

Besides the study of mesoscale meteorological processes, WIND was designed to be an airborne precursor experiment for a future satellite-borne Doppler lidar. An important step towards that goal was achieved, when the European Space Agency decided in 1999 to realize the Atmospheric Dynamics Mission (ADM) for measuring the global wind field (ESA 1999).

In conclusion, the presented results from the two WIND missions during the MAP SOP clearly demonstrate the instrument's ability to measure the wind field in a vertical plane below the aircraft with good accuracy. WIND is presently the only airborne instrument with a conical scanning technique to map the wind field from ground to flight level under clear-air conditions. It is envisaged that well coordinated further campaigns in close cooperation with mesoscale modelling teams will provide further insight into relevant dynamical processes from the synoptic scale down to the mesoscale.

Acknowledgements

The development of WIND was supported over the years by CNES, CNRS, Météo-France and DLR. The authors would like to thank all members of the joint WIND team from DLR and the Laboratoire de Météorologie Dynamique, especially Friedrich Köpp, Claude Loth, Engelbert Nagel, Bernard Romand, Jürgen Streicher, Stephan Rahm, Hartmut Herrmann, Ute Hauenstein, and the personnel of the DLR flight facility. We also thank Gerhard Gesell (DLR-DFD (Deutsches Fernerkundungsdatenzentrum)) for the processing of the Moderate Resolution Imaging Spectroradiometer (MODIS) data and Adrian Stannard (University of Reading) for ameliorating our foreigners' use of the English language. The data from the Milano sounding were taken from the MAP data centre at Eidgenössisches Technische Hochschule, Zurich. The Falcon missions during MAP were jointly funded by DLR and the US National Science Foundation. CNRS/Institut National des Sciences de L'Univers and Météo-France funded the French participation in MAP and the Institut du Développement et des Ressources en Informatique Scientifique provided computer resources under project 95059-CP1. DLR granted support for one co-author (Evelyne Richard) during an extended stay in Oberpfaffenhofen.

References

Bougeault, P., Binder, P., Buzzi, A., Dirks, R., Houze, R., Kuettner, J., Smith, R. B., Steinacker, R. and Volkert, H. 2001 The MAP Special Observing Period. *Bull. Am. Meteorol. Soc.*, **82,** 433–462

Browning, R. A. and Wexler, R. 1968 The determination of kinematic properties of a wind field using Doppler radar. *J. Appl. Meteorol.*, **7,** 105–113

Dabas, A., Werner, C., Delville, P., Reitebuch, O. and Drobinski, P. 2002 Observation of the wind field over a complex terrain during the field campaign ESCOMPTE: An application of the French–German airborne Doppler lidar WIND. Pp. 829–832 in *Lidar remote sensing in atmospheric and Earth sciences*. Eds. L. R. Bissonnette, G. Roy and G. Vallée. Library, Defence R&D Canada, 2459 Pie-XI Blvd North, Val-Bélair, QC G3J 1X5, Canada

Dabas, A., Drobinski, P., Reitebuch, O., Richard, E., Delville, P., Flamant, P. H. and Werner, C. 2003 Multi-scale analysis of a straight jet streak using numerical analyses and an airborne Doppler lidar. *Geophys. Res. Lett.*, in press

Dörnbrack, A., Leutbecher, M., Kivi, R. and Kyrö, E. 1999 Mountain-wave induced record low stratospheric temperatures above northern Scandinavia. *Tellus*, **51A,** 951–963

Dosio, A., Emeis, S., Graziani, G., Junkermann, W. and Levy, A. 2001 Assessing the meteorological conditions of a deep Italian Alpine valley system by means of a measuring campaign and simulations with two models during a summer smog episode. *Atmos. Environ.*, **35,** 5441–5454

Drobinski, P., Perin, J., Dabas, A. M., Flamant, P. H. and Brown, R. A. 2000 Simulation of the retrieval of a two-dimensional wave-like structure in the atmospheric boundary layer by an airborne 10.6 μm-heterodyne Doppler lidar. *Meteorol. Zeitschrift*, **9,** 329–338

Drobinski, P., Haeberli, C., Richard, E., Lothon, M., Dabas, A. M., Flamant, P. H., Furger, M. and Steinacker, R. 2003 Scale interaction processes during the MAP IOP 12 south föhn event in the Rhine Valley. *Q. J. R. Meteorol. Soc.*, **129,** 729–753

European Space Agency (ESA) 1999 'The four candidate Earth explorer core missions: Atmospheric dynamics mission'. ESA SP-1233 (4). ESA, c/o ESTEC, 2200 AG Noordwijk, the Netherlands

Flamant, C., Drobinski, P., Nance, L., Banta, R., Darby, L., Dusek, J., Hardesty, M., Pelon, J. and Richard, E. 2002 Gap flow in an Alpine valley during a shallow south föhn event: Observations, numerical simulations and hydraulic analogue. *Q. J. R. Meteorol. Soc.*, **128,** 1173–1210

Hunt, J. C. R. and Snyder, W. H. 1980 Experiments on stably and neutrally stratified flow over a model three-dimensional hill. *J. Fluid Mech.*, **96,** 671–704

Hollingsworth, A. 1994 Validation and diagnosis of atmospheric models. *Dyn. Atmos. Oceans*, **20,** 227–246

Lafore, J. P., Stein, J., Asencio, N., Bougeault, P., Ducrocq, V., Duron, J., Fisher, C., Héreil, P., Mascart, P., Masson, V., Pinty, J. P., Redelsperger, J. L., Richard, E. and Vila-Guerau de Arellano, J. 1998 The Meso-NH atmospheric simulation system. Part I: Adiabatic formulation and control simulations. *Ann. Geophys.*, **16,** 90–109

Pearson, G. N. and Collier, C. G. 1999 A pulsed coherent CO_2 lidar for boundary-layer meteorology. *Q. J. R. Meteorol. Soc.*, **125,** 2703–2721

Reitebuch, O., Werner, C., Leike, I., Delville, P., Flamant, P. H., Cress, A. and Engelbart, D. 2001 Experimental validation of wind profiling performed by the airborne 10μm-heterodyne Doppler lidar WIND. *J. Atmos. Oceanic Technol.*, **18,** 1331–1344

Rothermel, J., Cutten, D. R., Hardesty, R. M., Menzies, R. T., Howel, J. N., Johnson, S. C., Tratt, D. M., Olivier, L. D. and Banta, R. M. 1998 The multi-center airborne coherent atmospheric wind sensor. *Bull. Am. Meteorol. Soc.*, **79,** 581–599

Stein, J., Richard, E., Lafore, J. P., Pinty, J. P., Asencio, N. and Cosma, S. 2000 High-resolution non-hydrostatic simulations of flash-flood episodes with grid-nesting and ice-phase parameterization. *Meteorol. Atmos. Phys.* **72,** 203–221

Targ, R., Steakley, B. C., Hawley, J. G., Ames, L. L., Forney, P., Swanson, D., Stone, R., Otto, R. G., Zarifis, V., Brockman, P., Calloway, R. S., Klein, S. H. and Robinson, P. A. 1996 Coherent lidar airborne wind sensor. II: flight-test results at 2 and 10μm. *Appl. Opt.*, **35**, 7117–7127

Vaughan, J. M., Steinvall, O., Werner, C. and Flamant, P. H. 1996 Coherent laser radar in Europe. *Proc. IEEE*, **84**, 205–226

Volkert, H., Keil, C., Kiemle, C., Poberaj, G., Chaboureau, J.-P. and Richard, E. 2003 Gravity waves over the eastern Alps: A synopsis of the 25 October 1999 event (IOP 10) combining *in situ* and remote-sensing measurements with a high-resolution simulation. *Q. J. R. Meteorol. Soc.*, **129,** 777–797

Werner, C., Flamant, P. H., Reitebuch, O., Köpp, F., Streicher, J., Rahm, S., Nagel, E., Klier, M., Herrmann, H., Loth, C., Delville, P., Drobinski, P., Romand, B., Boitel, C., Oh, D., Lopez, M., Meissonnier, M., Bruneau, D. and Dabas, A. 2001 Wind infrared Doppler lidar instrument. *Opt. Eng.*, **40,** 115–125

Zardi, D., Gerola, R. and Tubino, M. 1999 'Measurement and modelling of a valley wind system in the Alps'. Pp. 28–31 in proceedings of the 13th conference on boundary layers and turbulence, Dallas, TX, USA. Am. Meteorol. Soc., Boston, USA